Available online at www.sciencedirect.com
ScienceDirect
Bioorganic & Medicinal Chemistry 15 (2007) 5752–5759
Bioorganic & Medicinal Chemistry

Inclusion complexes of pyrimethamine in 2-hydroxypropyl-β-cyclodextrin: Characterization, phase solubility and molecular modelling

Márcia Valéria Gaspar de Araújo,[a] Elze Kelly Barbosa Vieira,[a] Gilderman Silva Lázaro,[a] Leila de Souza Conegero,[b] Odair Pastor Ferreira,[b] Luís Eduardo Almeida,[a] Ledjane Silva Barreto,[a] Nivan Bezerra da Costa, Jr.[a] and Iara F. Gimenez[a,*]

[a]*Departamento de Química, Universidade Federal de Sergipe (UFS), Av. Marechal Rondon s/n, Campus Universitário Prof. José Aloísio de Campos, CEP 491000-000, São Cristóvão, SE, Brazil*
[b]*Instituto de Química, Universidade Estadual de Campinas (UNICAMP), Cidade Universitária Zeferino Vaz s/n, Caixa Postal 6154, CEP 13084-862, Campinas, SP, Brazil*

Received 10 March 2007; revised 31 May 2007; accepted 5 June 2007
Available online 12 June 2007

Abstract—The inclusion complexation of pyrimethamine in 2-hydroxypropyl-β-cyclodextrin has been investigated by 2D ^{1}H NMR, FTIR and UV/visible spectroscopy and also by molecular modelling methods (AM1, PM3, MM3). From the phase-solubility diagram a linear increase was observed in pyrimethamine aqueous solubility in the presence of 2-hydroxypropyl-β-cyclodextrin, evidencing the formation of a soluble inclusion complex. According to the continuous variation method (Job's plot) applied to fluorescence measurements, a 1:1 stoichiometry has been proposed for the complex. Concerning the structure of the complex, a Cl-in orientation of pyrimethamine in the 2-hydroxypropyl-β-cyclodextrin cavity has been proposed from the theoretical calculations, being confirmed by two-dimensional ^{1}H NMR spectroscopy (ROESY). The thermal behaviour has also been studied, providing complementary evidences of complex formation.

1. Introduction

Pyrimethamine (PYR), 5-(4-chlorophenyl)-6-ethyl-2,4-pyrimidineamine (Fig. 1) is a drug widely used in the treatment of parasitic diseases such as malaria and toxoplasmosis.[1] The mechanism of action of PYR is the inhibition of dihydrofolate reductase (DHFR), an essential enzyme responsible for the conversion of folic acid into folinic acid in the nucleic acid biosynthesis.[2] Some major drawbacks of PYR therapy include a relatively weak inhibitory activity and severe side effects such as nausea and neutropeny, which are caused by the low selectivity towards the parasite enzyme.[3] Additionally, owing to the low aqueous solubility of PYR high doses are necessary in order to provide a satisfactory inhibition of parasite proliferation. Efforts to overcome similar limitations presented by other drugs include the use of co-solvents, solubilizers, surfactants, and supramolecular hosts such as cyclodextrins.[4]

Cyclodextrins are cyclic oligosaccharides consisting of 6 (α-cyclodextrin), 7 (β-cyclodextrin), and 8 (γ-cyclodextrin) glucopyranose units linked by α-(1,4) bonds[5] (Fig. 2). The form of cyclodextrin molecules resembles truncated cones with the secondary hydroxyl groups located at the wider edge of the ring and the primary groups on the narrower edge. Hydrogen atoms are di-

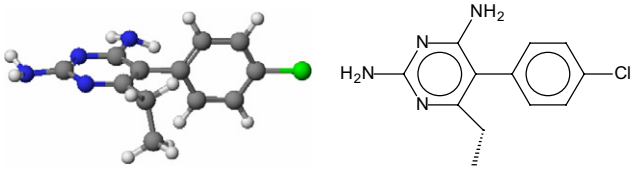

Figure 1. Spatial and plane representations of the PYR molecular structure.

Keywords: 2-Hydroxypropyl-β-cyclodextrin; Pyrimethamine; Inclusion complex; Toxoplasmosis.
* Corresponding author. Fax: +55 79 3212 6651; e-mail: gimenez@ufs.br

0968-0896/$ - see front matter © 2007 Elsevier Ltd. All rights reserved.
doi:10.1016/j.bmc.2007.06.013

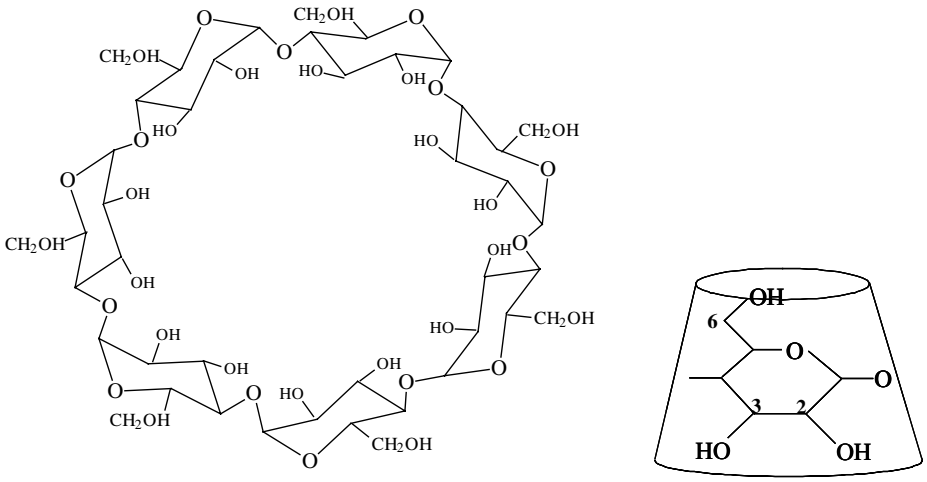

Figure 2. Representation of the front and side view of β-cyclodextrin molecule.

rected to the inner part of the ring resulting in a hydrophobic cavity along with a hydrophilic character outside the ring.[6] Hence cyclodextrins are soluble in water and at the same time may accommodate a broad range of hydrophobic species inside the cavity with formation of inclusion complexes. This property accounts for the great interest in cyclodextrins and it was shown that complex formation can be improved by chemical modifications of native cyclodextrins.[7]

2-Hydroxypropyl-β-cyclodextrin (HPBCD) is a hydroxyalkyl β-cyclodextrin derivative which is widely studied in the field of drug encapsulation owing to its inclusion ability along with a high water solubility.[8] In addition, toxicological studies pointed out that HPBCD is well tolerated by the human body both by intravenous and oral administrations.[9]

Here we report the preparation of an inclusion complex of PYR with 2-hydroxypropyl-β-cyclodextrin (HPBCD) in order to improve the aqueous solubility of the drug and to characterize the inclusion mode and stoichiometry of the inclusion complex. Molecular modelling calculations were also performed by molecular mechanics and semiempirical methods.

2. Results and discussion

2.1. Solubility studies

The determination of the phase-solubility diagram is a widely accepted method for evaluation of the effect of CD complexation on the drug solubility.[4] The 1:1 drug/cyclodextrin complex is the most common type of association where a single drug molecule is included in the cavity of one cyclodextrin molecule, with a stability constant $K_{1:1}$ for the equilibrium between the free and associated species. Figure 3 presents the phase-solubility diagram for the HPBCD/PYR system.

The solubility of the drug increased linearly as a function of the CD concentration, a feature of A_L-type com-

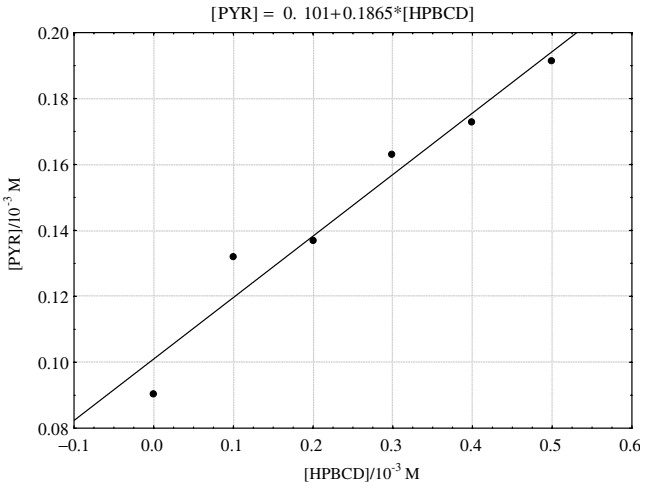

Figure 3. Phase-solubility diagram for the HPBCD/PYR system.

plexes, showing the formation of a water-soluble complex.[4] Also, a Slope lower than unit can be indicative of a 1:1 stoichiometry.[18] The apparent stability constant ($K_{1:1}$), calculated from a linear fit of the data, was found to be 1900.6 M^{-1} according to the following equation:

$$K_{1:1} = \frac{\text{Slope}}{\text{So}(1 - \text{Slope})}$$

where Slope is the value found in the linear regression and So is the solubility of the drug previously determined in the absence of HPBCD.[10] For the native cyclodextrins the observed values of $K_{1:1}$ are most often found between 50 and 2000 M^{-1},[11] thus the value found here indicates a high tendency of the drug to enter the HPBCD cavity. Some researchers argued that the apparent $K_{1:1}$ value must be analyzed with great care when a deviation between the value on the intercept from the linear fit (S_{int}) and So is present since the two values are supposed to be equal. In the present case we found that $(S_{int} - So)/S_{int}$ is 0.1 which is acceptable since strong deviations up to 30 are described.[11]

2.2. Stoichiometry of the complex

According to the continuous variation method, if a physical parameter directly related to the concentration of the complex can be measured for a set of samples with continuously variable molar fraction of components, the maximum concentration of complex will be present in the sample where the molar ratio R corresponds to the complexation stoichiometry. In Figure 4 the maximum fluorescence variation of PYR was observed for $R = 0.5$, which indicates that the main stoichiometry is 1:1, in agreement with the stoichiometry suggested from the phase solubility study.

2.3. Fourier-transform infrared spectroscopy (FTIR)

The FTIR spectra of HPBCD, PYR and the inclusion complex are shown in Figure 5 and the complete band assignments can be found in Table 1. In the spectrum of HPBCD none of the bands in the range 1500–400 cm^{-1} arise from a single type of molecular vibration due to a strong coupling of vibrations from the macrocyclic, caused by neighbouring bonds vibrating with similar frequencies.[12] The spectrum of the inclusion complex is dominated by the HPBCD bands by a combination of the following factors: (i) each HPBCD molecule has a relatively large number of polar groups (C—O, O—H, etc.), giving rise to intense absorption bands; (ii) both the host and guest molecules absorb coincidentaly in most of the spectral regions; (iii) there is an excess of free HPBCD in the inclusion complex sample. However, the presence of PYR is undoubtedly confirmed by the bands at 1570, 1558, 1261 and 802 cm^{-1}.

2.4. Molecular modelling and absorption spectra

In Table 2, we listed the enthalpies of both orientations obtained from the semiempirical methods (AM1 and PM3) and energies from MM3 method. The results indicate that the Cl-in orientation was more favourable than the Cl-out orientation from all theoretical methods. Semiempirical methods suggested the absence of H-bonds between the species, although the MM3 indicated

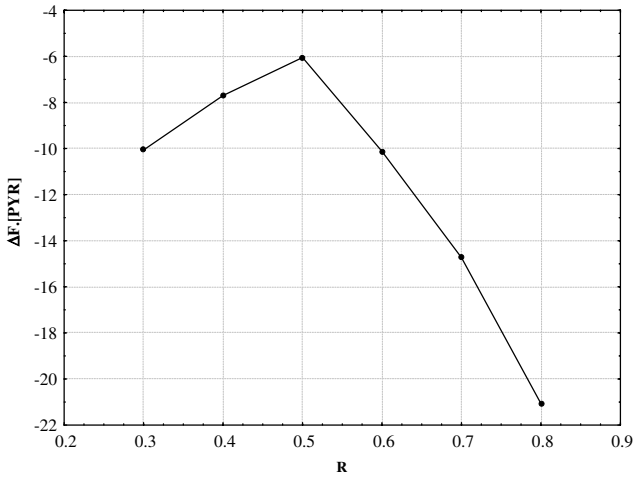

Figure 4. Continuous variation plot (Job's plot) for the HPBCD/PYR system from fluorescence measurements.

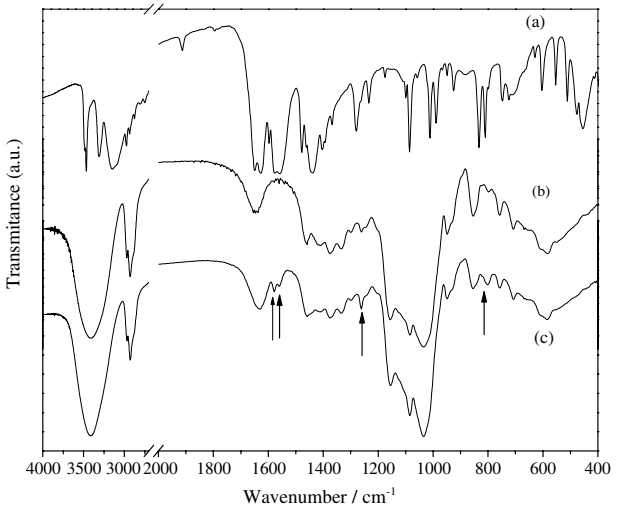

Figure 5. FTIR (Fourier-transform spectra) obtained in KBr disc for (a) PYR; (b) HPBCD and (c) HPBCD/PYR inclusion complex; bands marked with arrows are assigned to PYR.

the opposite, since the N–O distance from the nearest HPBCD hydroxyl is larger than 40 nm at semiempirical and is lower than 30 nm at MM3.

Figure 6 shows a comparison of theoretical and experimental absorption spectra for the Cl-in inclusion mode. All the theoretical spectra presented a small systematic blue shift, probably as a result of the calculation in vacuum. There are some differences between all calculated spectra, mainly near 230 nm, where both MM3 and PM3 yielded a medium intensity band, absent in the experimental spectrum. However, the spectrum calculated for the structure optimized with AM1 shows a better agreement with the experimental data. The Cl-in and Cl-out inclusion modes from AM1 are presented in Figure 7.

2.5. 2D NMR spectroscopy

2D ^{1}H NMR spectrum (ROESY) has become an important tool for the characterization of CD inclusion complexes, as the presence of NOE cross-peaks between protons from both species indicates separations closer than 0.4 nm in space. Also the relative intensities of cross-peaks depend on the distance between the corresponding protons. It is worth mentioning that few works show ROESY spectrum for HPBCD inclusion complexes. The use of derivatised cyclodextrins such as HPBCD brings complications to the interpretation of 2D NMR spectra and in some works a model complex with native β-CD is prepared for characterization. In such case an analogous inclusion mode is assumed on the basis of size similarity between cavities.[13]

Interactions to protons H-3 and H-5 of HPBCD, Figure 8a, are particularly important since these protons are located inside the cavity. Protons H-3 and H-5 in HPBCD present, respectively, chemical shifts of 3.923 ppm and 3.785 ppm. In the ROESY spectrum of the HPBCD/PYR inclusion complex, Figure 8b, it is possible to observe correlations of H-m protons (δ = 7.473 ppm – me-

Table 1. Wavenumbers (cm^{-1}) and assignments for the bands observed in the FTIR spectra of pyrimethamine and HPBCD

Infrared bands (cm^{-1}) and assignments	
Pyrimethamine	HPBCD
3467 and 3310: $\nu_{asym/sym}$(H—N—H) from NH_2	3410: ν(O—H)
3149: ν(C—H) from aromatic ring	2970 and 2930: ν(C—H)
1913 and 1793: combination bands from *p*-disubstituted aromatic rings	1458: δ(C—H) from CH_2 and CH_3
1600–1400: ν(C=C) e ν(C=N) from aromatic ring	1377: δ(C—H) from CH_3
1370: δ(C—H) from CH_3	1334: coupled δ(C—C—H), δ(C—O—H), δ(H—C—H)
1261: ν(C—N)	1261: coupled δ(O—C—H), δ(C—O—H), δ(C—C—H)
1100–980: in plane δ(C—H) from aromatic ring	1155 and 1080: coupled ν(C—O), ν(C—C), δ(C—O—H)
802: out of plane δ(C—H) from aromatic ring	1031: coupled ν(C—C), δ(O—C—H), δ(C—C—H), δ(C—C—O)
455: out of plane δ(C=C) from aromatic ring	948: skeletal vibration involving α-1,4 linkage
	850: coupled δ(C—C—H), ν(C—O), ν(C—C) from anomeric vibration

Wavenumber values and assignments for the HPBCD abd PYR in HPBCD/PYR inclusion complex are due to the same vibrational modes (see Section 2).
ν, stretching vibration; δ, bending vibration.

Table 2. Energies and formation enthalpy upon the inclusion complexation of HPBCD with PYR

HPBCD/PYR	Δ*E*/kcal/mol	$\Delta_f H$/kcal/mol	
	MM3	AM1	PM3
Cl-in	405.997	−1943.9	−1730.2
Cl-out	434.882	−1941.5	−1729.8
$X_{Cl\text{-}out} - X_{Cl\text{-}in}$ [a]	−28.885	−2.395	−0.400

[a] X is *E* for MM3 method and $\Delta_f H$ for semiempirical methods.

ta position relative to Cl) from the *p*-chlorophenyl moiety with H-5 and H-3 HPBCD protons. H-o protons (δ = 7.221 ppm) correlate mainly with H-5 HPBCD protons. We propose that the inclusion mode involves Cl-in orientation, with the PYR chloro-phenyl ring immersed into the cavity, in agreement to the AM1 optimized structure. This is similar to the inclusion mode described for the complex of *p*-chlorophenol in β-cyclodextrin,[14] which involves Cl-in mode with stronger correlations between both aromatic protons with H-5 and weaker correlations with H-3, evidencing a relatively deep penetration.

2.6. Differential scanning calorimetry and thermogravimetric analysis

The thermal behaviour of the inclusion complex was compared to that of the original species by TG and DSC measurements, Figure 9a–d. The DSC curve of PYR, Figure 9a, shows a sharp endothermic peak at 242 °C due to its melting with decomposition, since a mass loss was recorded from 190 °C in the TG curve. DSC curve of HPBCD, Figure 9b, exhibits two broad endothermic events in the ranges 75–175 °C and 240–340 °C, the first assigned to loss of water and the second one to thermal decomposition,[15] as the compound starts to lose mass in this range. The DSC curve of HPBCD/PYR physical mixture, Figure 9c, shows an apparent combination of events of both compounds: the broad signal centred near 100 °C, a broadened signal at 240 °C assigned to melting/decomposition of the drug, which could suggest the occurrence of some inclusion due to broadening, and above 320 °C the decomposition of the complex. Finally, the absence of PYR melting

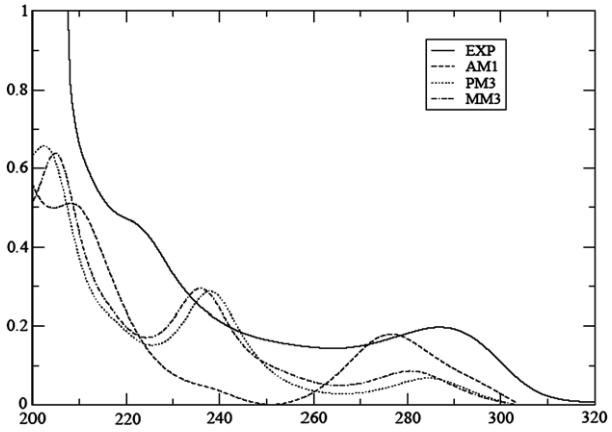

Figure 6. Absorption spectrum of complex PIR/HPBCD: experimental (EXP) and calculated in Cl-in orientation.

peak in the inclusion complex curve, Figure 9d, suggests the absence of PYR isolated crystals, which is consistent with inclusion. Also an increase in thermal stability of PYR can be suggested since the inclusion complex starts to decompose at temperatures higher than in the isolated form. This behaviour has been previously described as an evidence for encapsulation.[16]

2.7. X-ray diffraction analysis

The ordering degree in the structure of solid inclusion complex was compared to that of the parent solids by XRD measurements, Figure 10.

The powder XRD pattern of HPBCD, Figure 10a, presents only an amorphous halo due to its non-crystalline structure, in contrast to the presence of diffraction peaks in the diffractogram of crystalline PYR, Figure 10b. The diffractogram of the physical mixture HPBCD/PYR, Figure 10c, presents the typical PYR peaks in addition to the HPBCD halo. Finally both the inclusion complexes collected by evaporation and by freeze-drying, Figures 10d and e, respectively, present non-crystalline structures, indicating that the presence of guest molecules did not influence the typical HPBCD disordered packing. This observation is in agreement to previous

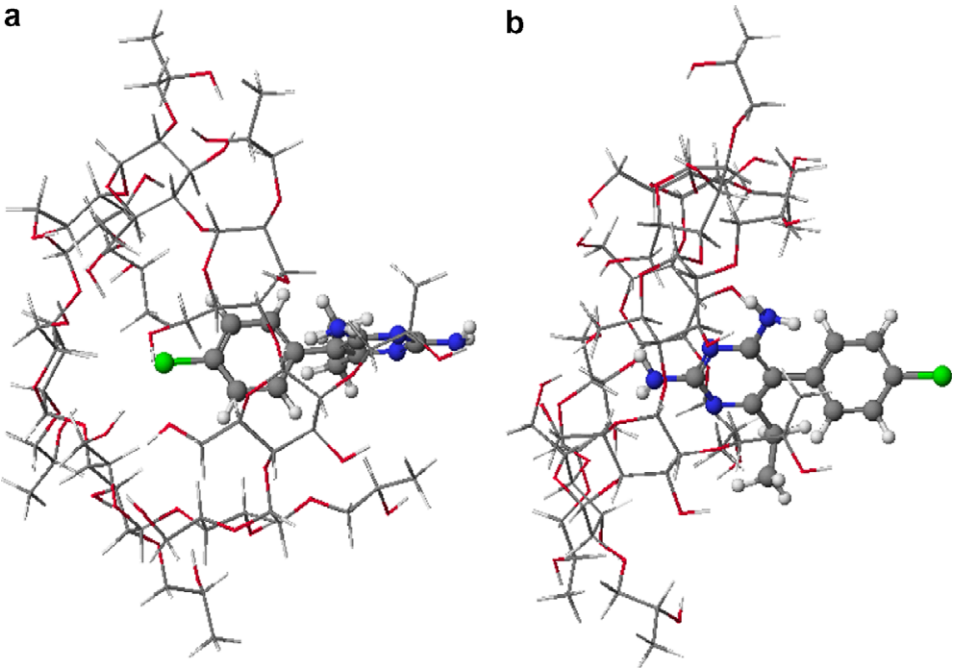

Figure 7. Complex PIR/HPBCD in two orientation: (a) Cl-in and (b) Cl-out.

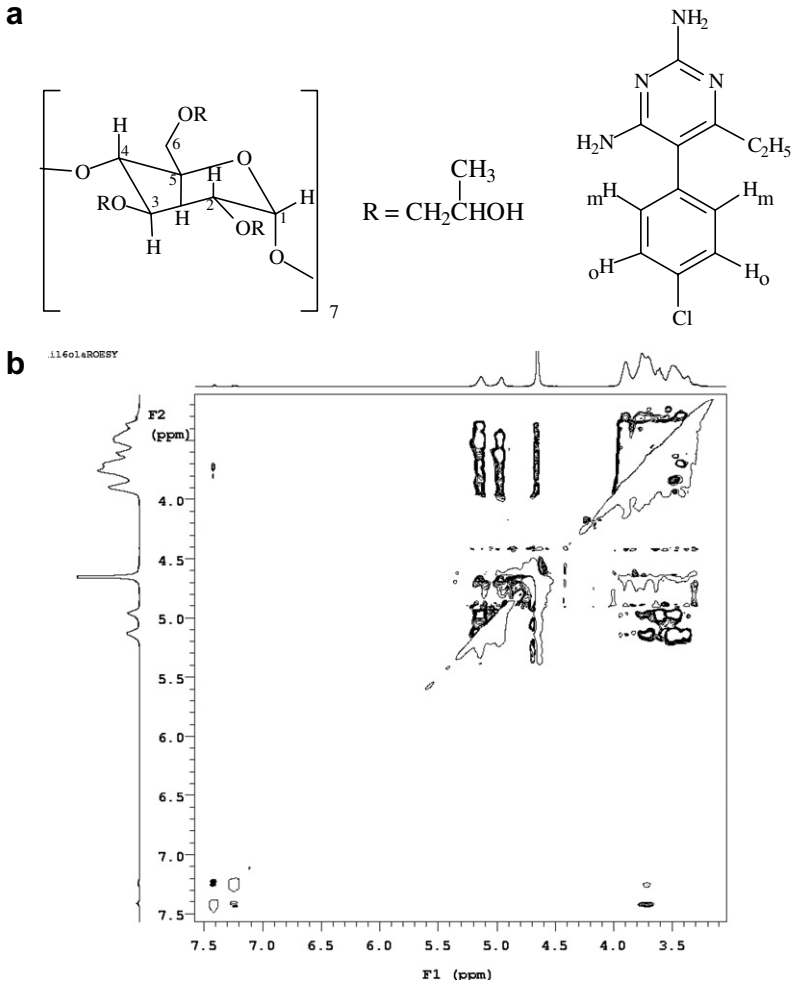

Figure 8. (a) Identification of HPBCD protons from the glucopyranose units (left) and of PYR aromatic protons (right); (b) ^{1}H ROESY spectrum of the system HPBCD/PYR in D_2O at 298.1 K with a mixing time of 200 ms.

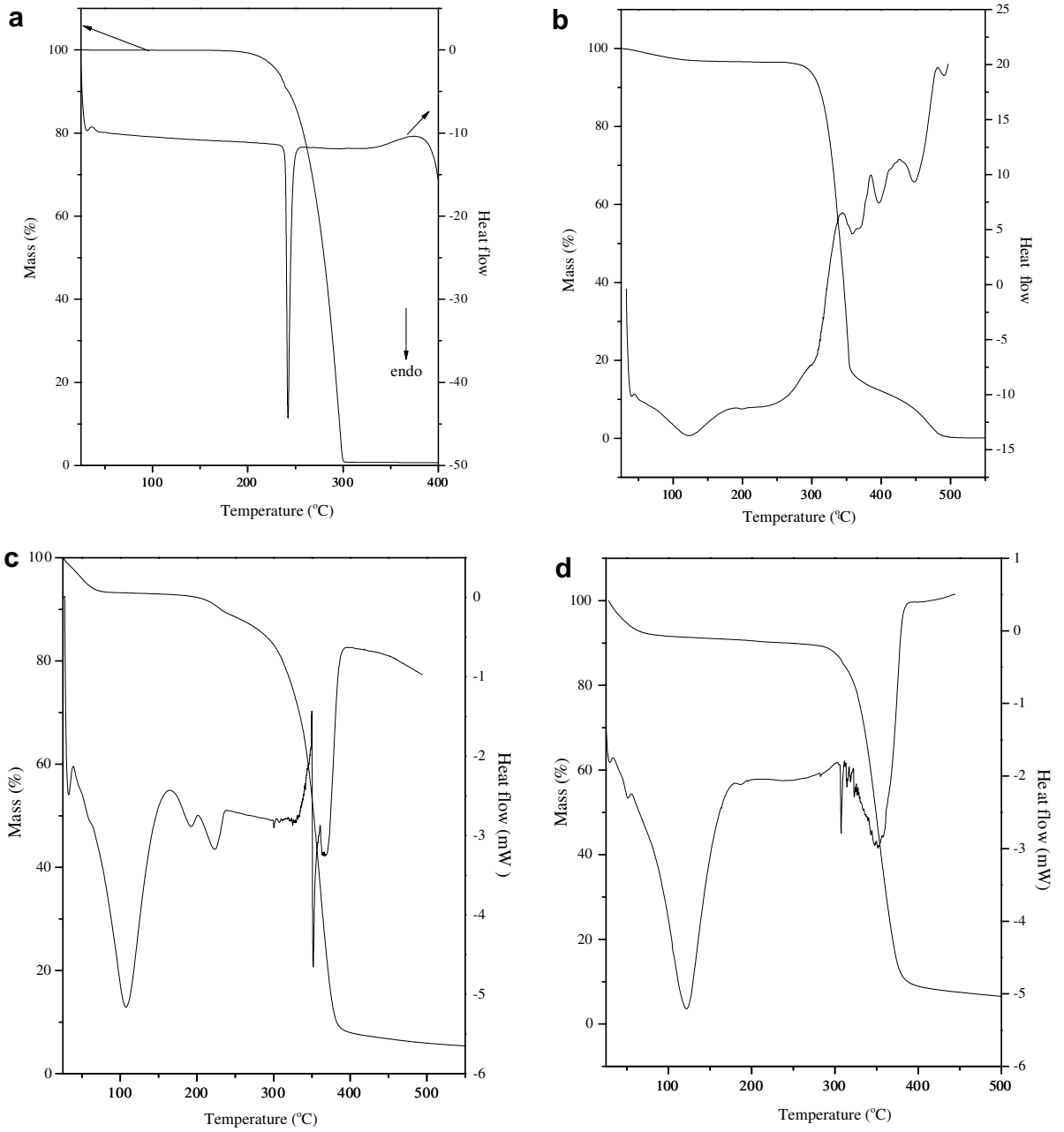

Figure 9. TG and DSC (N_2, 10 °C/min) curves for: (a) PYR; (b) HPBCD; (c) HPBCD/PYR 1:1(mol proportion) physical mixture, and (d) HPBCD/PYR inclusion complex.

reports of HPBCD inclusion complexes and is expected for the inclusion of small molecules[16] in non-crystalline cyclodextrin derivatives. Exceptions are some guests with large chains which form rotaxanes and polypseudo-rotaxanes with the cyclodextrins and induce some medium and long range order.[17]

3. Experimental

3.1. Materials

Pyrimethamine (mol wt 248.7) and 2-hydroxypropyl-β-cyclodextrin (mol. wt 1540) were purchased from Sigma. Other reagents and chemicals were of analytical reagent grade. All solutions were prepared using ultrapure water (MILLI Q).

3.2. Preparation of the inclusion complexes

Inclusion complexes were prepared by the suspension method. In a typical procedure, solid PYR was added to HPBCD aqueous solutions in the 1:1 molar proportion and the suspension was magnetically stirred at room temperature for 48 h protected from light. After the contact period the suspension was centrifuged at 15,000 rpm for 5 min and afterwards the liquid layer was filtered over 0.45 μm micropore membranes. The resulting solution was freeze-dried and alternatively dried in a rotary evaporator in order to collect the solid products.

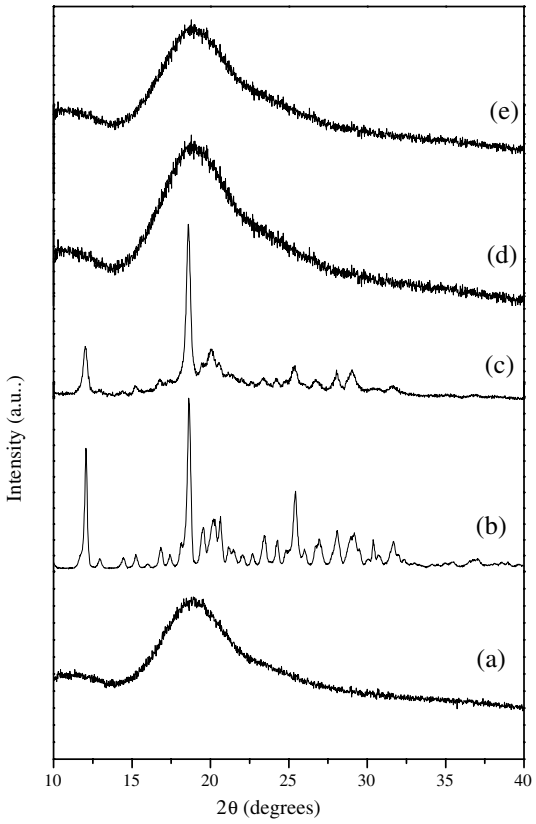

Figure 10. Powder X-ray diffractograms (Cu-κα) for: (a) HPBCD; (b) PYR; (c) HPBCD/PYR 1:1(mol proportion) physical mixture; (d) HPBCD/PYR inclusion complex collected by evaporation in rotary evaporator and (e) HPBCD/PYR inclusion complex collected by lyophilization.

Physical mixtures were also prepared by grinding together PYR and HPBCD in the 1:1 molar proportion in an agate mortar for 5 min.

3.3. Phase-solubility diagram

Phase solubility studies were carried out in aqueous medium according to Higuchi and Connors.[18] Briefly a five-fold molar excess of PYR—relative to the highest concentrated HPBCD solution—was added to aqueous HPBCD solutions of increasing concentrations (0.1, 0.2, 0.3, 0.4, and 0.5 mM). The mixtures were stirred for 48 h at room temperature protected from light, using a multipoint magnetic stirrer in order to provide similar stirring rates. After this period the suspensions were centrifuged at 15,000 rpm for 5 min, the upper liquid filtered over 0.45 μm micropore membranes and the absorbance read at 285 nm in a Perkin-Elmer Lambda 45 UV/vis spectrophotometer.

3.4. Stoichiometry determination by the continuous variation method (Job's plot)

The stoichiometry of inclusion was determined by the method developed by Job.[19] Equimolar 1.0×10^{-6} mol L^{-1} solutions of PYR and HPBCD were mixed to a standard volume (2 mL:8 mL; 3 mL:7 mL and so on) varying the molar ratio but keeping the total concentration of the species constant. An analogous dilution set of the PYR stock solution was carried out using ultrapure water. After stirring for 48 h, the fluorescence emission upon excitation at 285 nm (Perkin-Elmer LS 55 Luminescence Spectrometer) was measured for all solutions and $\Delta F = F - F_o$, the difference in fluorescence intensity in the presence and in the absence of HPBCD, was plotted against R; R = [PYR]/{[PYR]+[HPβCD]}.

3.5. Characterization of the inclusion complexes

The samples collected in solid state were characterized as follows. FTIR spectra were obtained in KBr discs using a Perkin-Elmer BX instrument with 4 cm^{-1} spectral resolution; thermal analysis (thermogravimetry—TG and differential scanning calorimetry—DSC) was performed using TA instruments models 2960 and 2010, respectively, both with 10 °C/min heating rates and under 100 mL/min N_2 flow; powder X-ray diffraction (XRD) was measured in a Rigaku diffractometer using Cu κα (λ = 1.5406 Å) with 40 mA, 40 kV and scanning rate of 3°/min. Rotating-frame Overhauser effect spectroscopy (ROESY) experiment was carried out in a Varian INOVA spectrometer at 500 MHz using D_2O as solvent, relaxation delay 2.0 s and mixing time = 2.00 ms.

3.6. Molecular modelling—geometry optimization and calculation of the transition energies

Two different inclusion orientations were considered: the first one with chlorine pointing towards the HPBCD cavity (Cl-in) and the other with the opposite NH_2 group pointing (Cl-out) towards the cavity. The inclusion complex was emulated by entering the guest molecule from one end of the HPBCD molecule and then letting it pass through the host molecule by steps. Dihedral angles between PYR rings were changed stepwise using MM3 method. The minimum energy structure was found, without any constraint, with semiempirical (AM1, PM3)[20] and MM3 force field[21] methods implemented within the Cache Worksystem 6.1[22] program. The electronic excited state calculations have been performed with the intermediate neglect of differential overlap/spectroscopic parametrization–configuration interaction singly replacements (INDO/S-CIS) method[23] implemented within the ZINDO[24] program. The inclusion complex was held in the positions determined by each method. The line broadening of the calculated single transition energies and the intensities obtained from oscillator strengths were taken into account by fitting them to a Lorentzian line shape function with a half-height band width of 20–40 nm, which properly allows the comparison between the calculated and the observed absorption electronic spectra.

Acknowledgments

The authors are grateful to Prof. O.L. Alves and L. Otubo from LQES-IQ-Unicamp, and to Prof. I.O. Mazali from IQ-Unicamp. E.K.B.V. acknowledges to CAPES for fellowship.

References and notes

1. Bosch-Driessen, L. H.; Verbraak, F. D.; Suttorp-Schulten, M. S. A.; van Ruyven, R. L. J.; Klok, A. M.; Hoyng, C. B.; Rothova, A. *Am. J. Ophthalmol.* **2002**, *134*, 34.
2. Anderson, A. C. *Drug Discov. Today* **2005**, *10*, 121.
3. Katlama, C.; De Wit, S.; O'Doherty, E.; van Glabeke, M.; Clumeck, N. *Clin. Infect. Dis.* **1996**, *22*, 268.
4. Davis, M. E.; Brewster, M. E. *Nat. Rev. Drug Discov.* **2004**, *3*, 1023.
5. Szejtli, J. *Chem. Rev.* **1998**, *98*, 1743.
6. Martin Del Valle, E. M. *Process Biochem.* **2004**, *39*, 1033.
7. Khan, A. R.; Forgo, P.; Stine, K. J.; D'souza, V. T. *Chem. Rev.* **1998**, *98*, 1977.
8. Gould, S.; Scott, R. C. *Food Chem. Toxicol.* **2005**, *43*, 1451.
9. Fromming, K. H.; Szejtli, J. Pharmacokinetics and Toxicology of Cyclodextrins. In *Proc. of the 8th Int. Symposium on Cyclodextrins*, Szejtili, J., Szente, L. Eds., 1996.
10. Lazaro, G. S., Master Thesis, UFS, 2006.
11. Loftsson, T.; Hreinsdóttir, D.; Másson, M. *Int. J. Pharm.* **2005**, *302*, 18.
12. Egyed, O. *Vibrat. Spectrosc.* **1990**, *1*, 225.
13. Spamer, E.; Müller, D. G.; Wessels, P. L.; Venter, J. P. *Eur. J. Pharm. Sci.* **2002**, *16*, 247.
14. Leyva, E.; Moctezuma, E.; Strouse, J.; Garcia-Garibay, M. A. *J. Incl. Phenom. Macrocyc. Chem.* **2001**, *39*, 41.
15. Veiga, M. D.; Merino, D.; Lozano, R. *J. Therm. Anal. Calorim.* **2002**, *68*, 511.
16. Liu, Y.; Chen, G.-S.; Chen, Y.; Lin, J. *Bioorg. Med. Chem.* **2005**, *13*, 4037.
17. Yang, Y.-W.; Chen, Y.; Liu, Y. *Inorg. Chem* **2006**, *45*, 3014.
18. Higuchi, T.; Connors, K. A. *Adv. Anal. Chem. Instrum.* **1965**, *4*, 117.
19. Dewar, M. J. S.; Zoebisch, E. G.; Healy, E. F.; Stewart, J. J. P. *J. Am. Chem. Soc.* **1985**, *107*, 3902.
20. Stewart, J. J. P. *J. Comput. Chem.* **1989**, *10*, 209.
21. Allinger, N. L.; Yuh, Y. H.; Lii, J. H. *J. Am. Chem. Soc.* **1989**, *111*, 8551.
22. CAChe 6.0—Fujitsu, Ltd, Chiba, Japan.
23. Popple, J. A.; Beveridge, D. L.; Dobosh, P. A. *J. Chem. Phys.* **1967**, *47*, 2026.
24. Zerner, M. C. *Zindo Package, Quantum Theory Project*; Williamson Hall University: Florida, 1990.